Improving 3D Shape Recognition with Electrostatic Friction Display

Reza Haghighi Osgouei, *Student Member, IEEE*, Jin Ryong Kim, *Member, IEEE*, and Seungmoon Choi, *Senior Member, IEEE*

Abstract—Electrovibration technology has the potential for seamless integration into ordinary smartphones and tablets to provide programmable haptic feedback. The aim of this work is to seek effective ways to improve 3D perception of visual objects rendered on an electrovibration display. Utilizing a gradient-based algorithm, we first investigated whether rendering only lateral frictional force on an electrovibration display improves 3D shape perception compared to doing the same using a force-feedback interface. We observed that although users do not naturally associate electrovibration patterns to geometrical shapes, they can map patterns to shapes with moderate accuracy if guidance or context is given. Motivated by this finding, we generalized the gradient-based rendering algorithm to estimate the surface gradient for any 3D mesh and added an edge detection algorithm to render sharp edges. Then, we evaluated the advantages of our algorithm in a user study and found that our algorithm can notably improve the performance of 3D shape recognition when visual information is limited.

Index Terms—Electrostatic friction display, electrovibration, shape, rendering, recognition

1 Introduction

Touchscreens are versatile devices that can display visual content and receive touch input, but they lack the ability to provide programmable tactile feedback. This limitation has been addressed by a few approaches generally called surface haptics technology. This technology modulates the friction between a user's fingertip and a touchscreen surface to create different tactile sensations when the finger explores the touchscreen. This functionality enables the user to see and feel digital content simultaneously, leading to improved usability and user experiences.

One major approach in surface haptics relies on the electrostatic force induced between the finger and an insulating surface on the touchscreen by supplying high AC voltage [1], [2], [3]. The use of AC also induces a vibrational sensation called electrovibration to the user. Electrostatic friction displays require only electrical components and provide uniform friction over the screen. This tactile feedback technology not only allows easy and lightweight integration into touchscreen devices [4], [5] but also provides dynamic, rich, and satisfactory user interfaces [1], [2].

This work was motivated during our on-going research to integrate an autostereoscopic 3D visual display using multi-focal planes and an electrostatic friction display into one touchscreen device. Multi-focal plane displays provide superior 3D visual perception than regular displays, and we have been seeking methods to further enhance 3D perception by means of haptic feedback. Such multimodal interaction may expand the mainly horizontal interaction space of touchscreen also to the depth direction, providing more natural and intuitive 3D interaction. In the rest of this section, we review related work and then present an overview and contributions of this work.

- *R. H. Osgouei and S. Choi are with the Haptics and Virtual Reality Laboratory, Department of Computer Science and Engineering, Pohang University of Science and Technology (POSTECH), Pohang, Gyeongbuk 790-784, Republic of Korea. E-mail: {haghighi, choism}@postech.ac.kr.*
- *J. R. Kim is with the Electronics and Telecommunications Research Institute, Daejeon, Republic of Korea. E-mail: jessekim@etri.re.kr.*

Manuscript received 1 Oct. 2016; revised 18 May 2017; accepted 25 May 2017. Date of publication 1 June 2017; date of current version 13 Dec. 2017. (Corresponding author: Reza Haghighi Osgouei.)
Recommended for acceptance by F. Giraud.
For information on obtaining reprints of this article, please send e-mail to: reprints@ieee.org, and reference the Digital Object Identifier below.
Digital Object Identifier no. 10.1109/TOH.2017.2710314

1.1 Related Work

1.1.1 Rendering 3D Features on a Flat Display

There has been relatively little work as to rendering 3D features using only lateral forces on a flat surface. The sandpaper system of Minsky et al. [6], the first pioneering work in this line of research, reported that lateral forces applied to the user exploring a simulated surface can deliver the perception of small bumps and dents. They introduced a gradient-based technique for texture rendering that computes 2D elastic lateral force from the local gradient of surface height and renders the force using a 2D force-feedback joystick. Later, perceptual studies conduced by Robles-De-La-Torre and Hayward [7] applied the same idea to large-scale features such as bumps and holes. They demonstrated that in active exploration of a physical shape, lateral force applied to the sliding finger plays the main role in shape perception. Using a 1D force-feedback device without visual cues, different combinations of physical and virtual geometries (bump, hole, and flat surface), e.g., a virtual bump laid on a physical flat surface, were presented to participants. Although the virtual shapes were rendered using only lateral force, the participants could accurately identify the virtual shapes.

Recently, Kim et al. applied the same idea of gradient-based rendering to express 3D features on a touchscreen using electrovibration [2]. They first compared users'

preference for three types of force profile (height, slope, and rectangular) for a visual bump displayed on the screen. Results indicated that the slope (gradient) profile best matched the visual bump. They generalized this finding to a 2D gradient-based rendering algorithm for 3D features on an image and then applied the algorithm to many user interface examples. However, no assessments were made as to the performance of this algorithm in improving the perception of 3D features. This is in contrast to [7], which clearly demonstrated that participants *haptically* perceived 3D features from gradient-based lateral force rendering.

1.1.2 Electrostatic Friction Display

The phenomenon of electrovibration was first introduced by Mallinckrodt et al. [8]. They accidentally discovered that an insulated surface supplied with an AC voltage source elicits a rubber-like sensation when the surface is scanned by the finger. This phenomenon is due to the electrostatic attraction force between two conductive plates separated by a dielectric. When the finger scans an insulated electrode, a condenser is formed between the electrode and the conductive substance under the skin. Exciting the electrode using a periodic voltage induces electrostatic attraction, and this increases the friction force between the surface and the moving finger. This electrostatic stimulation was introduced into a tactile display by Strong et al. [9]. They developed the first electrostatic display using a stimulator array consisting of a large number of small electrodes. Later, a polyimide-on-silicon electrostatic fingertip tactile display was fabricated with 49 electrodes arranged in a square array [10].

These early findings have recently been elaborated for application to touchscreens, beginning with TeslaTouch [1]. TeslaTouch was the first electrostatic tactile display on a touchscreen using a capacitive touch panel (Microtouch, 3M, USA [11]) as the core component. The panel is made of a thick glass layer on the bottom, a transparent electrode (indium tin oxide; ITO) in the middle, and a thin insulator layer on the top. In the usual setup, the electrode is excited by high AC voltage, and the human body is grounded electrically. The same panel has been used by many other researchers since then [2], [3], [12], [13], [14], [15].

Some other researchers developed their own electrovibration display not using the 3M capacitive touch panel. Pyo et al. built a tactile display that provides both electrovibration and mechanical vibration on a large surface [16]. They fabricated an insulated ITO electrode on top of an electrostatic parallel plate actuator, both operating based on the electrostatic principle. A non-transparent electrostatic friction display was also developed in [17], [18] using an aluminum plate covered with a thin plastic insulator film.

These displays do not support multi-touch or localized friction modulation, and all fingers in contact with the surface experience the same sensation. This issue was addressed by several prototypes presenting local stimulation. For example, a display panel was developed with multiple horizontal and vertical ITO electrodes in a grid enabling localized stimulation at the region where the vertical and horizontal electrodes cross each other [19]. In [20], a multi-finger electrostatic display was developed consisting of a transparent electrode and multiple contact pads on which users place their fingers. Applying different voltages to the pads and electrically grounding the transparent electrode induce different frictional stimuli to the multiple fingers.

Whereas electrovibration requires high AC driving voltage, a recent alternative relies on *electroadhesion*. This technology can generate large electrostatic force between a finely-polished coated metallic surface and a fingertip when excited by a high DC voltage [21]. The output force is more unified and less vibratory, but the technology requires more complex hardware without a transparent version yet.

1.1.3 Device Calibration

The relationship between input signal and output friction in electrostatic friction displays is not completely understood, and a number of studies have shown great interest in defining such relationship. Researchers have worked on this topic either by measuring friction forces using a tribometer [12], [18] or by estimating perceived intensities in psychophysical experiments [2], [22]. For instance, Meyer et al. [12] developed a tribometer to make precise measurements of finger friction and confirmed the expected square law of frictional force to driving voltage. They also showed a linear mapping between friction and normal force, confirming the Coulombic model of dry friction. Conducting a six-value effect strength subjective index rating, Wijekoon et al. showed a significant correlation (0.8) between signal amplitude and perceived intensity but no correlation between frequency and perceived intensity [22]. In [2], participants assigned a number between 0 and 100 to the subjective friction intensity. A linear fit in log-log scale was observed in the normalized results relating applied voltage amplitude to perceived friction force intensity. Kang et al. studied driving methods for lower input voltage while preserving the perceptual strength of electrovibration [23]. Vardar et al. investigated the effect of input voltage waveform on the perception of electrovibration and found that a human finger is more sensitive to low frequency square waves than sinusoidal waves [24].

1.2 Research Overview

The aim of our work has been finding effective methods for improving 3D shape perception of visual objects displayed on a touchscreen by providing frictional haptic feedback. For that, we first present the physical characteristics of the electrostatic friction display used in our research (Section 2). Then we address a fundamental question to our research: Can users identify 3D features, such as bumps and holes, from electrovibration feedback alone without any visual information? To answer this question, we conducted a formative user study (Section 3) using a gradient-based lateral force rendering algorithm adapted from the literature [2], [6], [7].[1] This study showed that users cannot naturally associate electrovibration patterns to 3D shapes without visual cues, but they can with acceptable performance if explicit guidance is given.

Based on this finding, we have generalized the basic gradient-based lateral force rendering algorithm to work with 3D mesh models (Section 4). This extended algorithm casts a ray to find the surface point touched by the user's finger and then computes the gradient using the current and previous contact points. The force command to an electrostatic friction display is computed using both the gradient and the device input-output characteristics. This mesh rendering algorithm also includes an additional edge emphasis step to render sharp edges more clearly. Finally,

1. This formative user study was presented earlier in the 2016 IEEE Haptics Symposium [25].

we conducted a summative user study to quantify the performance improvement of 3D shape recognition enabled by our algorithm under limited visual conditions (Section 5).

The contributions of our work can be elucidated by comparison with the work of Kim et al. [2], which is based on the same idea of gradient-based rendering for 3D features in [7]. First, in the user study in [2], participants' task was to choose one force profile (out of three) that was perceived the most consistent with a visual Gaussian bump. The goal was to determine which force profile to use in their rendering algorithm, and participants selected the slope (gradient-based) profile most frequently. Whereas this certainly fit to the purpose, it remained unknown what 3D geometry the participants actually elicited from the force profile and how accurate the association was. In contrast, our formative user study was designed to answer these questions, and it evaluated the extent to which gradient-based rendering using electrovibration can elicit the perception of 3D features without any visual guidance. This better reflects the capability of haptic device and rendering algorithm and also unveils the nature of the haptic percepts users feel more clearly. Second, while the rendering algorithm described in [2] is for images, our generalized rendering algorithm is for 3D meshes. Third, we also report a summative user study in order to validate the advantages of our mesh rendering algorithm using an electrostatic friction display. In [2], however, no such user studies were conducted (instead many example applications were demonstrated).

2 Device Characterization

In this study, we used a Feelscreen development kit (Senseg, Finland) as the electrostatic friction display, which comprises an electrostatic film overlaid on a commercial tablet (Google Nexus 7). Its software development kit (SDK) supports nine haptic effects (called haptic grains) that provide noticeably different friction patterns. The temporal properties of the haptic grains are fixed, but their intensity can be controlled using a normalized value (0.0–1.0). However, the Feelscreen SDK does not allow completely-customable input, e.g., a sinusoidal wave with a given frequency and amplitude, and the characteristics of generated friction forces were unknown. Hence, it was necessary to characterize FeelScreen's various haptic grains, and we built a rotary tribometer for that purpose.

2.1 Tribometer

Our tribometer is similar to those used in previous work [12], [18], but also has a few differences. The previous studies required great care in controlling the electrical skin impedance of fingertip since it depends greatly on person, temperature, and moisture. In particular, the skin moisture level can change even in a short period of use. We found that the electrostatic display of Feelscreen also responded to some touch pens. The sensations of electrovibration resulted from the use of such a touch pen and the bare finger were very similar. Hence, our tribometer uses a touch pen instead of the human fingertip for data collection for precise regulation of measurement conditions. Our tribometer is also rotary for a simpler mechanical design whereas the previous ones used linear scanning movements.

Our tribometer consists of a DC motor (RB-35GM, DnJ, Korea) with a touch pen attached to its shaft using a holder and a six-axis force/torque sensor (Nano 17, ATI Technologies, USA) placed under the tablet (Fig. 1). The length of the pen holder is 6 cm, which makes the rotation radius 3 cm. A balancing beam with a counterweight on the opposite end of the touch pen is used to adjust the normal pressure. The beam is pivoted at the middle to provide free vertical movement. The counterweight mass ($\simeq 470$ g) is selected to approximate the normal pressure of human hand. The rotation velocity ($\simeq 6.5$ cm/s) is chosen for the usual human hand velocity during surface scanning. The force data is sampled at 10 KHz using a 16-bit data acquisition board (NI USB-6251, National Instruments, USA).

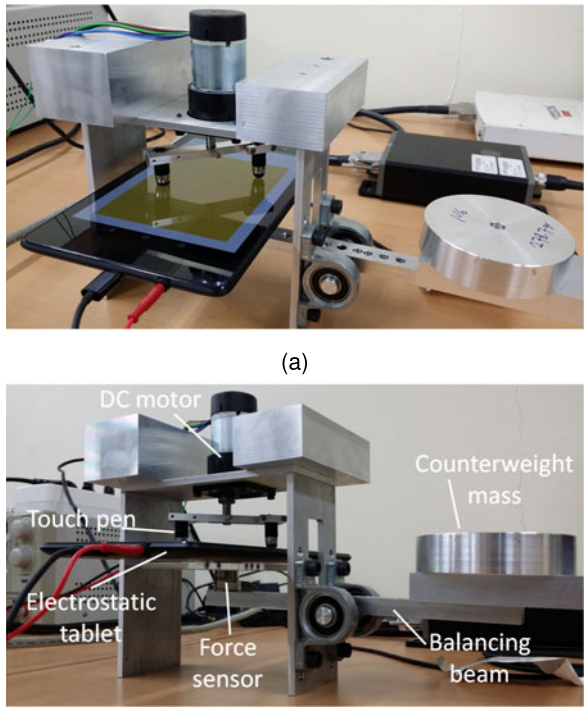

Fig. 1. Rotary tribometer. (a) Top view. (b) Bottom view.

2.2 Input-Output Characteristics

To characterize the dynamic behavior of the Feelscreen device, we used a ruled scanning surface as shown in Fig. 2a. Whenever the touch pen, rotating along the dashed circular path, crossed one of the straight lines, electrovibration was activated. In each trial, we collected 20 seconds of data and then applied a Butterworth band-pass filter with a low cut-off frequency of 10 Hz and a high cut-off frequency of 500 Hz. Fig. 2b shows an example of tangential force collected from a haptic grain named EDGE-SOFT (provided in the Feelscreen SDK) with the maximum intensity of 1.0. It also reveals that whenever a line was crossed by the touch pen, a vibratory tangential force occurred with a peak-to-peak (p-p) amplitude as large as 0.25 N.

We then identified the relationship between input intensity and the magnitude of output tangential force. For each intensity between 0.1 and 1.0 (step size 0.1), we collected force data and applied the same band-pass filter. We computed the p-p amplitude of the tangential force and then averaged the 50 largest values. The mean p-p amplitude showed a quadratic relationship to the input intensity, as shown in Fig. 2c (haptic grain EDGE-SOFT). Assuming the internal

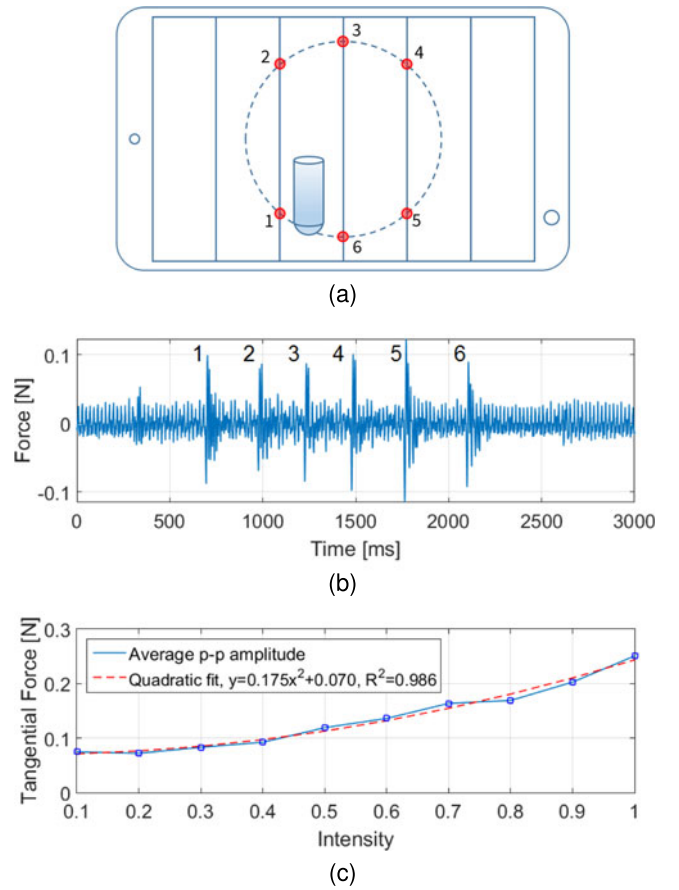

Fig. 2. Dynamic behavior of the electrostatic friction display. (a) Ruled scanning surface consisting of equally spaced straight lines. The touch pen rotates along the circular path (dashed line) crossing each line twice. The cross points are marked with red circles and numbered from 1 to 6. (b) Filtered lateral force. The peaks in the signal are numbered matching the cross points. (c) Peak-to-peak amplitude of tangential force versus input intensity with a quadratic fit.

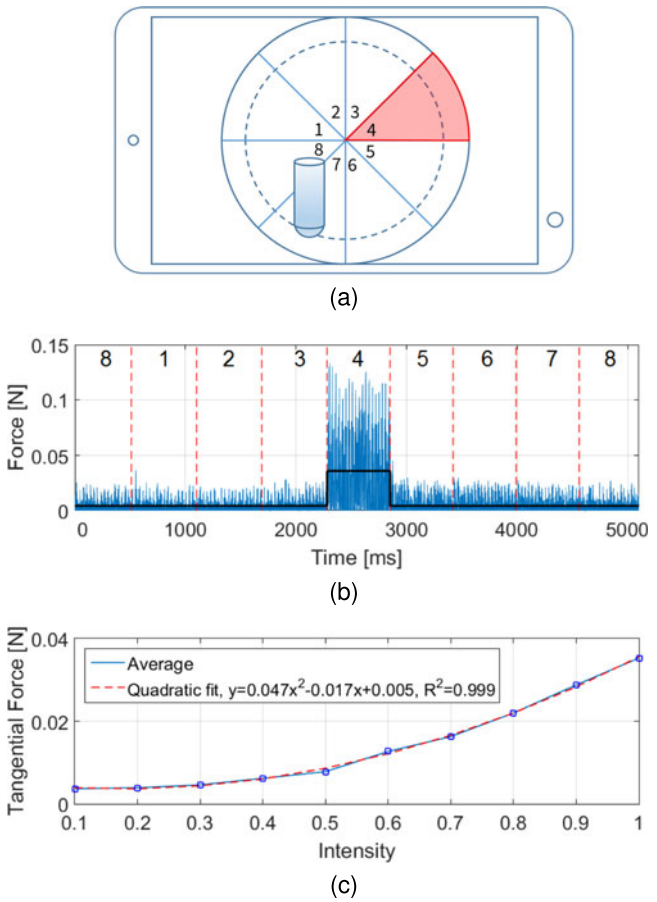

Fig. 3. Static behavior of the electrostatic friction display. (a) Circular scanning surface. When the touch pen passes over the (red) highlighted area (circular sector 4), electrovibration is enabled. (b) Filtered tangential force (blue). The data were averaged to estimate the static friction force increase (black). The numbered intervals correspond to the sectors in (a). (c) Static friction force increase versus input intensity showing a good quadratic fit.

amplification unit of Feelscreen has a constant gain, the relationship between its input (grain intensity) and output (voltage applied to the electrostatic film) should be be linear. Based on this assumption, the obtained result conforms to the classic theory of electrovibration that the output force magnitude is in proportion to the square of input voltage [8].

We also looked at the static behavior of friction force using a different Android application rendering a circular scanning surface (Fig. 3a) The circular surface was divided to eight equal circular sectors, and the EDGE-SOFT haptic grain was enabled for only one circular sector (number 4, highlighted red in Fig. 3a) and disabled for the other sectors. For measurements, the touchpen was rotated on the surface by our tribometer.

An exemplar plot of filtered lateral forces is given in Fig. 3b. We also computed average forces when electrovibration was on and off (black line in Fig. 3b) and used their difference to represent the increase of static friction force. This procedure was repeated for each input intensity between 0.1 and 1.0 (step size). The average increases of static friction force are shown in Fig. 3c as a function of input intensity. The relationship was quadratic again, as was for the vibratory friction force.

We also provide time domain and FFT plots of four haptic grains used in the formative and summative studies (Fig. 4). The lateral forces were measured using our tribometer from a scanning surface on which the corresponding haptic grain was played continuously. For the time domain plots, only 2 seconds of data are shown for visibility, but the whole data were used to compute the FFTs.

Lastly, we can sample the finger position using the capacitive touchscreen at the maximum sampling rate of about 100 Hz and update the haptic grain command in our Android programs. The internal analog signal reconstruction rate of FeelScreen is however unknown although it is much faster than 100 Hz.

3 Formative User Study

This formative user study aimed to assess how well users can recognize primitive 3D geometrical shapes when provided with depictions of the shapes by the friction force produced by an electrostatic display. A similar method was also implemented using a force-feedback haptic interface for inclusion in the experiment as the baseline.

3.1 Force Profiles

Following [7], we designed two basic 3D geometries, a Gaussian bump and hole, as well as a flat surface. The Gaussian profiles had a length of 5 cm and a height of

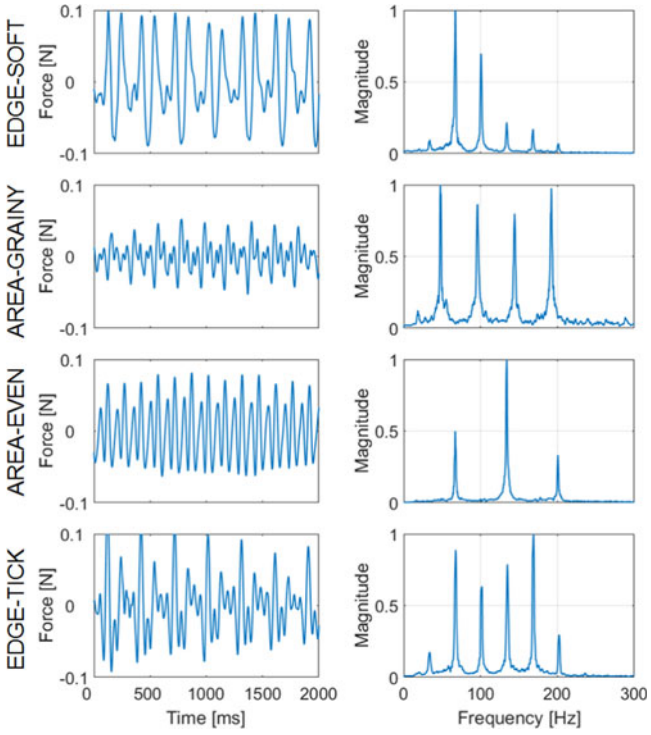

Fig. 4. Time domain (left) and FFT plots (right) of four haptic grains used in the formative and summative studies.

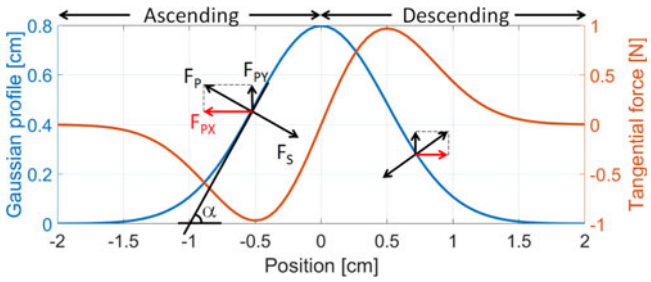

Fig. 5. Gaussian bump (blue) and the corresponding force profile (red) taken from [7]. The scanning direction is from left to right.

0.8 cm. They were computed using (1) with $\mu = 0$ and $\sigma = 0.5$,

$$y(x) = \frac{1}{\sqrt{2\pi}\sigma}\exp\left(-\frac{(x-\mu)^2}{2\sigma^2}\right). \quad (1)$$

An exemplar Gaussian bump is shown in Fig. 5. The bumps and holes had a width of approximately 2.6 cm.

3.1.1 For Force-Feedback Device

To compute force profiles for Gaussian bumps and holes, we followed the procedure described in [7]. Assume that the user applies force $\mathbf{F_s}$ at position $\mathbf{p}(x, y)$ when exploring a frictionless physical surface (Fig. 5). Then the surface returns $\mathbf{F_p} = -\mathbf{F_s}$. $\mathbf{F_p}$ can be decomposed to F_{px} and F_{py}, the tangential and normal components to the scanning surface, such that

$$\begin{aligned} F_{px} &= -F_{py}\tan(\alpha(x)), \\ \tan(\alpha(x)) &= \frac{dy}{dx} = -\frac{1}{\sigma^2}xy, \end{aligned} \quad (2)$$

where $\alpha(x)$ is the angle of $\mathbf{p}(x, y)$.

TABLE 1
Experimental Conditions for Force-Feedback and Electrovibration Devices

Condition	Force-feedback	Electrovibration
1	FF-BUMP-FR	EV-BUMP-IP0.5-HG1
2	FF-BUMP-FF	EV-BUMP-IP0.7-HG1
3	FF-HOLE-FR	EV-BUMP-IP0.5-HG2
4	FF-HOLE-FF	EV-BUMP-IP0.7-HG2
5	FF-FLAT	EV-HOLE-IP0.5-HG1
6		EV-HOLE-IP0.7-HG1
7		EV-HOLE-IP0.5-HG2
8		EV-HOLE-IP0.7-HG2
9		EV-FLAT-HG1
10		EV-FLAT-HG2

FF: force feedback and EV: electrovibration.
FR: friction-based algorithm and FF: force field-based algorithm.
IP: intensity profile and HG: haptic grain.

The normal force F_{py} applied by the user was measured using a force sensor in [7]. However, impedance-type force feedback devices and electrostatic displays generally do not have force or pressure sensors. Hence, we assumed 1 N for F_{py}, based on pilot experiments. An example tangential force profile for a Gaussian bump is plotted in Fig. 5. When scanned from left to right, the tangential force F_{px} resists movement during ascent and assists movement during descent. The force changes its direction when the slope is zero at the summit of the bump.

A computer program was developed using CHAI3D to render the computed force profiles with a force-feedback device using force field and friction algorithms, respectively. In the force field-based algorithm, the tangential force profile (force values between −1.0N and 1.0N) is directly sent to the force-feedback device. In the friction-based algorithm, the dynamic friction coefficient of a virtual surface is adjusted based on the force profile using a mapping (IP0.5, force values between 0N and 1.0N) explained in Section 3.1.2.

Five experimental conditions were formed by combining three geometries (bump, hole, and flat surface) and the two rendering algorithms (force field-based and friction-based); see a summary in Table 1. Only the friction-based algorithm was used for the flat surface.

3.1.2 For Electrostatic Display

Tangential force profiles for a force-feedback device contain both positive (resisting movement) and negative (assisting movement) forces. However, an electrostatic display cannot render active forces to assist movement, and this is the fundamental limitation of passive friction displays. We handle this problem by linearly mapping the normalized force from −1.0 N to 1.0 N to the input intensity of the Feelscreen tablet from 1.0 to 0.0; this maps -1.0 N to the maximum friction, 0 N to the middle intensity friction, and 1.0 N to the minimum friction (of the touchscreen itself). This is the same technique used in [2]. Since the input intensity profile has an offset of 0.5, we call this method IP0.5 (Figs. 6a and 6c). A similar mapping was also used to implement the friction-based rendering for force-feedback devices.

The device characterization results in Fig. 2c showed that the actual electrostatic friction for input intensity 0.5 is lower than 50 percent of the full scale force. The

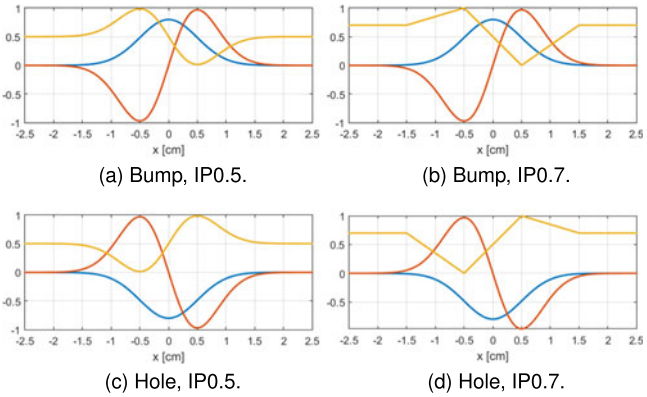

Fig. 6. Profiles for the electrostatic display. Blue: geometry [cm], red: force [N], and orange: intensity.

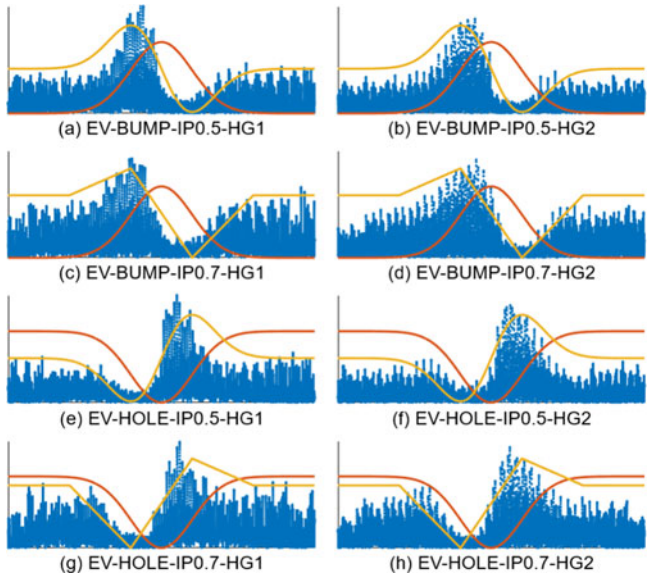

Fig. 7. Measured friction force profiles for each experimental condition. Blue: measured force profile [N] (only absolute values are shown for clarity), red: geometry profile, orange: intensity profile (scaled to show the trend). The x-axis is for time, and the y-axis is for force amplitude. Force amplitudes are normalized to show clear agreement between rendered and measured profiles.

minimum friction force is about 0.075 N and the maximum is 0.25 N, with the median 0.16 N occurring at about 0.7 of input intensity. This was basis for another intensity profile IP0.7 using 0.7 as the offset. For mapping, we approximate the Gaussian force profiles with piecewise linear intensity profiles for simplicity (Figs. 6b and 6d), which does not cause noticeable perceptual differences, e.g., between the smooth Gaussian IP0.5 and its piecewise linear version. These profiles were rendered using an Android application we developed.

The experiment consisted of ten experimental conditions, combining three geometries (bump, hole, and flat surface), two intensity profiles (IP0.5 and IP0.7), and two haptic grains (HG1: EDGE-SOFT and HG2: AREA-GRAINY; chosen after pilot experiments); see Table 1. We included the two haptic grains since they rendered quite different sensations (EDGE-SOFT: smooth and AREA-GRAINY: rough; see Fig. 4). A constant force profile with maximum intensity 1.0 was used for the flat surface. The electrovibration stimuli measured using the tribometer are shown in Fig. 7 for the eight experimental conditions containing bumps and holes. The geometry and intensity profiles are also shown for reference. It is clear that the induced electrostatic friction forces match with their corresponding intensity profiles. The friction force patterns of bumps and holes are clearly distinguishable. Considering the square law from input intensity to output friction force (Section 2), the friction forces rendered using IP0.7 resulted in more symmetric profiles than those rendered using IP0.5.

3.2 Participants

Twelve participants (9 male, 3 female; M 22.7 years, SD 2.6 years) were recruited for this study. None reported noteworthy previous experiences using kinesthetic haptic interfaces or electrostatic displays. They signed an informed consent form prior to the experiment. Each participant was paid 10,000 KRW (9 USD) after the experiment.

3.3 Procedure

In the experiment, we used a PHANToM (1.0A; Geomagic, USA) as a force-feedback device and the Feelscreen tablet as an electrostatic display. Participants were randomly divided into two groups. The participants in group G1 first performed the five experimental conditions with the PHANToM, and then the ten experimental conditions with the Feelscreen tablet; see Table 1. This was switched for the participants in group G2. The order of the experimental conditions for the PHANToM and that for the Feelscreen tablet were randomized for each participant.

For each device, the experiment consisted of two parts. Part 1 was for open descriptions; participants were asked to freely describe their percept and experience in writing after exploring each stimulus. Nothing was provided to participants that could bias their perception. Part 2 was for a closed question; for each stimulus, participants were asked to choose one of the following four answers: 1) bump, 2) hole, 3) flat surface, and 4) none of these. They were instructed to select the shape that best described their percept. Part 1 was performed first, followed by Part 2 using the same device after a short break.

During the experiment, the haptic device was placed inside a box to which the participants had frontal access. A curtain covered the box to prevent participants from obtaining any visual cues. The experimenter could see the device from the back of the box and provided occasional guidance to the participant's pose and scanning speed when necessary. For the experiment with the Feelscreen tablet, participants were asked to hold the touch pen vertically and scan the surface from left to right. Each of the ten experimental conditions was presented only once. For the experiment with the PHANToM, the same touch pen was attached to the last vertical link of the PHANToM, and a seven-inch tablet was placed under the touch pen to provide similar scanning experiences. Participants were asked to hold the touch pen vertically and scan the surface from left to right. Each of the five experimental conditions was repeated twice. The numbers of bumps, holes, and flat surfaces were not known to participants to prevent guessing based on counting.

Prior to the experiment, participants were given enough time to practice and become familiar with the system. During the experiment, they were allowed to rest when

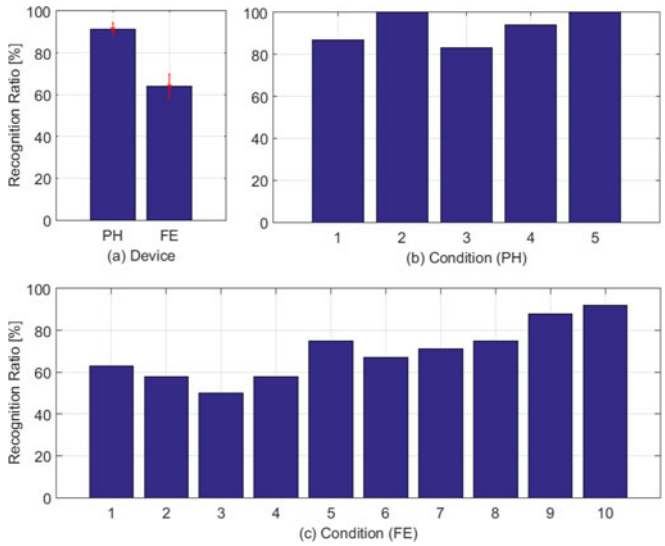

Fig. 8. (a) Correct recognition ratios using the PHANToM (mean = 91 percent) and the Feelscreen tablet (mean = 64 percent). Error bars show standard errors. (b) Correct recognition ratios with the PHANToM for each experimental condition (see Table 1). (c) Correct recognition ratios with the Feelscreen tablet for each experimental condition (see Table 1).

necessary. Participants' scanning velocity and vertical pressure were not controlled; they were free to adjust the velocity and pressure for better perception. The experiment took approximately one hour to finish for each participant.

3.4 Results

3.4.1 Open Descriptions

We compiled the participants' answers collected in the first part of the experiment. No noticeable differences were observed between the participants of group G1 and G2.

Most of the participants described the sensations provided by lateral force feedback using geometrical terms. Frequently used words included bump, hole, protrusion, groove, convex or concave shape, ascent, and descent. Only one participant did not use any geometry-related term and instead used material-related terms, e.g., spring. These results reinforce the previous finding of [7] that lateral force alone can render clearly identifiable 3D primitives.

For the surfaces rendered using electrovibration, the majority of the participants described their sensations with terms related to vibration and friction, and sometimes texture. Only one participant mentioned a geometrical term (hole). It appears that electrovibration alone is not able to elicit strong illusions of perceiving 3D geometric shapes.

The time the participants spent to complete each experimental condition was shorter with the PHANToM than the Feelscreen tablet. After three or four scans with the PHANToM, the participants began to write down their descriptions, while the Feelscreen required six or seven scans.

3.4.2 Closed Selections

The average correct recognition ratios of geometric shapes computed for the two devices are shown in Fig. 8a. The correct recognition ratio for each device was calculated by dividing the total number of correct answers from all participants received in each experimental condition by the total number of responses in that condition. The most important result is that the recognition performance with the Feelscreen tablet was 64 percent. This value indicates that when the participants were given explicit guidance, they could associate the electrovibration patterns to the primitive 3D shapes at much above the chance level (25 percent), with statistical significance (right-tailed t-test; $p < 0.001$). However, the recognition performance was much lower than that with the PHANToM (91 percent).[2] We also checked the performance difference between the two participant groups G1 and G2 using the Kruskal-Wallis test, but it was not statistically significant ($p = 0.88$). Overall, the experimental results allows a mild promise that well-designed gradient-based algorithms for an electrostatic friction display would improve the perception of 3D visual objects displayed on a touchscreen.

Additionally, Fig. 8b shows the average correct recognition ratios measured with the PHANToM for each experimental condition.[3] On average, bumps were recognized more correctly than holes (94 versus 89 percent; compare the ratios of condition 1 and 2 with those of condition 3 and 4). The force field-based algorithm showed higher performance than the friction-based algorithm (97 versus 85 percent; condition 1 and 3 versus condition 2 and 4).

The mean correct recognition ratios measured with the Feelscreen tablet are shown in Fig. 8c for each experimental condition. The most prominent observation is that holes (conditions 5–8) were more often correctly identified than bumps (conditions 1–4) with 72 versus 57 percent correct recognition ratios, respectively. The performance difference caused by the two intensity profiles was negligible (IP0.5 66 versus IP0.7 65 percent), and so was the recognition accuracy difference between the two haptic grains (HG1 69 versus HG2 70 percent).

Any comparisons in the two preceding paragraphs cannot be proven statistically with our present experimental design. They must be taken as preliminary observations.

3.4.3 Discussion

First, if no guidance or context implying association to geometric shapes is provided, users cannot identify primitive 3D features from electrovibration alone. Second, when a clue about the geometric shapes is given, users can associate electrovibration patterns to geometric shapes at well above the chance level. The performance, however, is below the best performance achieved with active force feedback.

Frictional feedback using electrovibration has two important differences from active force feedback. First, it conveys clear sensations of vibration, as predominantly mentioned by the participants. This can be a major reason that preclude users from associating electrovibration patterns with geometric shapes unless guided explicitly. Second, electrovibration does not allow the rendering of active tangential forces

2. The correct recognition ratios measured using the PHANToM did not follow a normal distribution (the ratios were very high and bounded above by 100 percent). Thus, rank-based tests should be used for statistical tests to examine the effect of haptic device, and we used the Kruskal-Wallis test for that in our previous conference paper [25]. However, we recently learned that such treatment was inadequate and no suitable rank-based tests exist because the data measured with the PHANToM included repeated measures but those measured with the Feelscreen did not. Therefore, we no longer include the statistical comparison between the two haptic devices reported in [25].

3. Only one ratio was computable for each experimental condition. Hence no error bars are shown in Figs. 8b and 8c. No statistical tests were performed for the same reason.

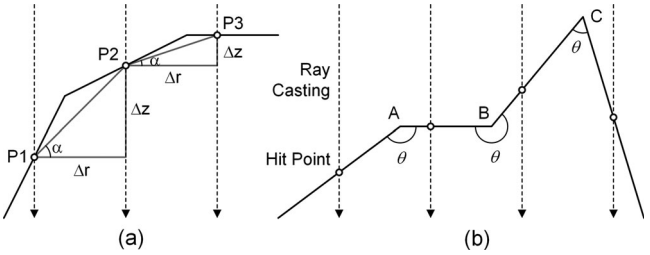

Fig. 9. (a) Variables for the generalized lateral force rendering algorithm. (b) Dihedral angles. Thick lines represent the cross-section of polygons.

that assist movement. Although we imitated this behavior using only friction, the effectiveness of that approach seems to have a limit.

The similar performance between the two haptic grains HG1 and HG2 is an indication that type of haptic grain is not a main factor for geometry recognition, although they may provide different sensations. Delivering noticeable friction fluctuations according to the intensity profile appears to be sufficient. The same can be said to the effect of intensity profile, based on the similar recognition ratios of the two intensity profiles IP0.5 and IP0.7.

4 Generalized Gradient-Based Lateral Force Rendering Algorithm

The formative user study indicated that electrostatic friction displays have the potential to render 3D features by modulating friction force according to the gradient of the profile if sufficient context is provided. However, the algorithm used was for the explicit representation of the profile. This motivated us to generalize the basic algorithm implemented for the formative user study to cover general 3D objects modeled using meshes, as detailed in this section.

4.1 Basic Algorithm

Suppose that a user explores a 3D object displayed on a touchscreen by scanning it with a finger. We call the finger's position a touch point (x, y) defined in the 2D touchscreen coordinates. For lateral force feedback, this 2D touch point is mapped to the 3D touch point (x, y, ∞) in the 3D world coordinate frame of the 3D object. From each 3D touch point, a vertical ray is cast along the z-direction toward the 3D object for collision detection. If any collisions are detected, we take the collision point with the greatest height (z-coordinate) and call it a hit point for the ray.

We estimate the surface gradient that the user's finger experiences by computing the linear slope between the two consecutive hit points of the current and previous frames. Let the current hit point be $P2 = (x_2, y_2, z_2)$ and the previous hit point be $P1 = (x_1, y_1, z_1)$ in Fig. 9a. Then the surface gradient at $P2$ is approximated by

$$\tan(\alpha) = \frac{\Delta z}{\Delta r}, \tag{3}$$

$$\Delta z = z_2 - z_1, \tag{4}$$

$$\Delta r = \sqrt{(x_2 - x_1)^2 + (y_2 - y_1)^2}. \tag{5}$$

Recall that the lateral force is obtained from

$$F_{pxy} = -F_{pz} \tan(\alpha). \tag{6}$$

With $F_{pz} = 1$ N as in the formative user study,

$$F_{pxy} = -\frac{\Delta z}{\Delta r}. \tag{7}$$

As we have shown earlier, the relation between input intensity and output force is quadratic. Also to preserve force direction, we consider a signed square root of lateral force as follows:

$$F^{sq} = \mathrm{sgn}(F_{pxy})\sqrt{|F_{pxy}|}, \tag{8}$$

and then map F^{sq} to the input intensity I.

An important issue here is that F^{sq} can have an arbitrary value depending on the object geometry and the scanning direction and velocity of the user's finger, but the tangential force that an electrostatic display can generate is limited. Hence, we need to assume that F^{sq} is also bounded, i.e., $F^{sq}_{min} \le F^{sq} \le F^{sq}_{max}$, and then linearly map this interval into to the input intensity $I \in [1.0, 0.0]$ of the haptic grain to generate. Note that F^{sq}_{min} (resisting force; note its sign) must provide the maximum friction ($I = 1.0$) by the electrostatic display whereas F^{sq}_{max} (assisting force) should exert the minimum friction ($I = 0.0$). This can be elaborated by considering the empirical observation that I lower than 0.3 does not produce perceptually clear lateral force. That is, we linearly map F^{sq} in $[F^{sq}_{min}, F^{sq}_{max}]$ to I in [1.0, 0.3]:

$$I = \frac{0.7F^{sq} + 0.3F^{sq}_{min} - F^{sq}_{max}}{F^{sq}_{min} - F^{sq}_{max}}. \tag{9}$$

If $F^{sq} \le F^{sq}_{min}$, $I = 1.0$, and if $F^{sq} \ge F^{sq}_{max}$, $I = 0.3$.

4.2 Computing Minimum and Maximum Force

The generalized lateral force rendering algorithm is straightforward, but how to determine $(F^{sq}_{min}, F^{sq}_{max})$ requires some careful considerations. In the formative user study, $F^{sq}_{min} = -1$ and $F^{sq}_{max} = 1$ since the minimum and maximum of lateral force F_{px} were -1 N and 1 N, respectively, for the 2D Gaussian profiles. In general 3D cases, minimum and maximum lateral forces cannot be obtained easily. They depend on the scanning direction and speed of the user's finger and also the geometry of the 3D object. If $(F^{sq}_{min}, F^{sq}_{max})$ is not set properly, the rendering will use either a narrow range of I or the minimum or maximum friction excessively, being unable to express the geometric changes of the 3D object appropriately.

To determine an effective range for $(F^{sq}_{min}, F^{sq}_{max})$, we simulate the haptic rendering process by scanning the object with various velocities and directions. This process results in a large number of F^{sq} values. Then we use $(F^{sq}_{min}, F^{sq}_{max}) = (\mu - 2\sigma, \mu + 2\sigma)$, where μ is the mean and σ is the standard deviation. This corresponds to the 95 percent confidence interval if F^{sq} follows a Gaussian distribution.

We empirically confirmed that this simple method generally works well for many 3D models. It is also demonstrated in the summative user study in Section 5. There can also be good alternatives depending on the distribution of F^{sq}.

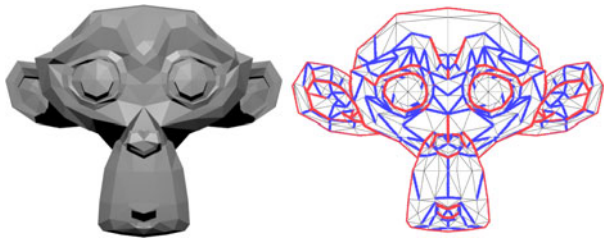

(a) (b)

Fig. 10. (a) 3D mesh of a Monkey model. (b) Results of edge emphasis. All convex edges are highlighted in blue. Among them, those with $\theta < 135^\circ$ (relatively sharp ones) are marked in red.

4.3 Edge Emphasis

The generalized lateral force rendering algorithm provides haptic feedback regarding the convexity or concavity of a 3D object. However, sharp edges on the surface may be rendered inadequately if their neighbor faces result in F^{sq} close to F^{sq}_{min} or F^{sq}_{max}, or outside $(F^{sq}_{min}, F^{sq}_{max})$. In such cases, the device output is saturated, and the lateral force rendering algorithm alone cannot render sharp tactile sensations for the edges. To remedy this problem, we detect the edges of a 3D object and emphasize them as follows.

Many edge detection algorithms are available in computer vision and graphics [26], [27], and those taking a mesh as input are pertinent to our purpose [28]. Most of such algorithms are based on the notion of *dihedral angle*: the angle between two planes that share an edge. Dihedral angle roughly approximates the principle curvature of the surface at the edge [29]. An edge with a dihedral angle greater than a given threshold is considered as a sharp edge.

In parallel with the gradient-based lateral force calculation, we also compute at each frame the dihedral angle θ from the polygon to which the previous hit point belongs to the polygon on which the current hit point lies. θ can be easily calculated from the normal vectors of the two polygons. An edge is convex if $\theta < 180^\circ$ (A and C in Fig. 9b) and concave if $\theta > 180^\circ$ (B in Fig. 9b). We consider only convex edges since concave ones are not reachable in reality. Further, a convex edge becomes sharper if the dihedral angle θ is decreased from 180° to 0° (compare A and C in Fig. 9b). Hence, we represent the sharpness S of a convex edge by

$$S = -\frac{\theta - 180^\circ}{180^\circ - \theta_{min}}, \tag{10}$$

where θ_{min} is the smallest dihedral angle of the object. This function maps $\theta = 180^\circ$ to $S = 0$ and $\theta = \theta_{min}$ to $S = 1$.

To emphasize convex edges, we play a haptic grain of different type (EDGE-TICK) with intensity I_e. This is in comparison to the AREA type haptic grain (AREA-EVEN) used for surface profile rendering. The two haptic effects generate easily distinguishable frictional stimuli (Fig. 4). I_e is determined by linearly mapping the sharpness S to the intensity interval [0.3, 1.0],

$$I_e = 0.7S + 0.3. \tag{11}$$

An example of edge emphasis is given in Fig. 10.

5 Summative User Study

We conducted another user study to evaluate the effectiveness of our generalized gradient-based lateral force rendering algorithm. The task was to recognize 3D objects presented to the user with limited visual information. This task was motivated by the finding of the formative user study that frictional electrovibration can deliver 3D geometric information if its context is explicit to users. Some visual stimuli were designed to be difficult for visual recognition. Our aim was to assess the extent to which our electrovibration rendering algorithm can facilitate the recognition task in such situations. This study was approved by the IRB of POSTECH (PIRB-2016-E015).

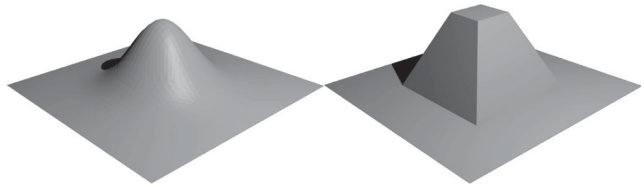

(a) (b)

Fig. 11. 3D shapes used in the summative user study. (a) Gaussian bump: width 6, length 6, height 1.8, $z(x, y) = \frac{8}{1.4\pi}\exp(\frac{-x^2-y^2}{1.4})$. (b) Square frustum bump: width 6, length 6, height 2, base square 3×3, top square 1×1. All dimensional units are cm.

5.1 Methods

5.1.1 Stimuli

We used two 3D objects, bumps and holes, each in two different profiles, Gaussian and square frustum, in this experiment (Fig. 11). Detailed equation and dimension are given in Fig. 11 for the bumps. The holes were made by inverting the corresponding bumps.

One visual scene consisted of four bumps and holes, but their profiles were the same (all Gaussians or frustums). Varying the numbers of bumps and holes resulted in five different configurations (Fig. 12): 0B4H (0 bump and 4 holes), 1B3H (1 bump and 3 holes), 2B2H (2 bumps and 2 holes), 3B1H (3 bumps and 1 hole), and 4B0H (4 bumps and 0 hole). Which were bumps or holes out of the four positions was determined randomly for each configuration, but once made the same scene was used for all participants. For example, in configuration 1B3H, a bump can be placed in one of the four locations (top-left, top-right, bottom-left, bottom-right). We chose to fixe the bump to top-right (for Gaussian scenes) and to bottom-right (for square frustum scenes). This was to keep the size of the experiment manageable. We also confirmed that similar visual information was presented regardless of the positions of bumps and holes.

To limit visual information, we controlled several design factors as follows: 1) Orthographic projection was used to render the 3D scenes. A perspective projection may provide sufficient visual information for object identification; 2) Only the top view was shown to the user. Looking at objects from other angle may enable sufficient visual information even with orthographic projection; 3) Two lighting conditions were applied: a vertical spotlight and a directional light rotated (45, 45, 0 degree) around the $x - y - z$ axes. They create very different shadows depending on the object configuration in the scene. 4) All objects were rendered in gray; and 5) No textures were added to the objects. Combining all these factors, 20 (= 2 shapes $\times$ 2 lights $\times$ 5 configurations) different scenes were designed (Fig. 12).

5.1.2 Participants

Twenty participants (14 male, 6 female; M 22.7 years old, SD 3.0 years) were recruited for this study. They were divided

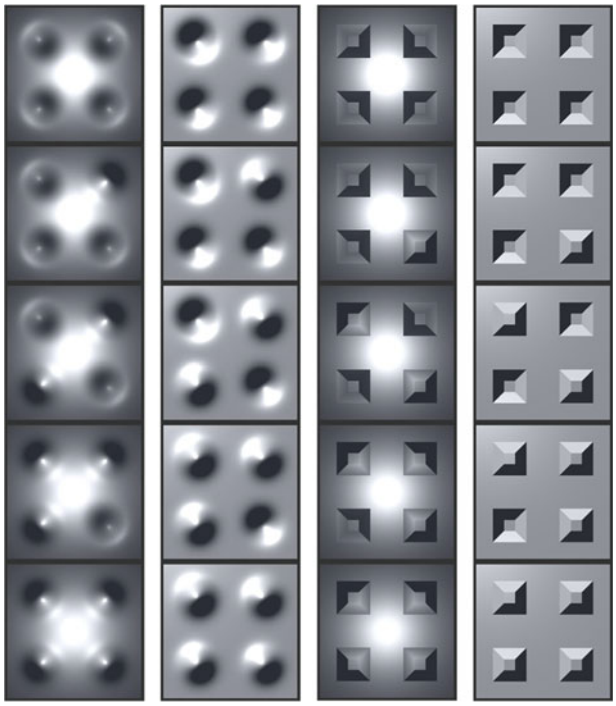

Fig. 12. Experimental conditions. Twenty scenes were composed by combining two shapes (Gaussian and square frustum), two lighting conditions (spotlight and directional), and five configurations (0B4H, 1B3H, 2B2H, 3B1H, and 4B0H). From left to right: Gaussian-spotlight, Gaussian-directional light, square frustum-spotlight, and square frustum-directional light. From top to bottom: 0B4H, 1B3H, 2B2H, 3B1H, and 4B0H. Some scenes can be easily confused because the direction of directional light in not known to users. For instance, the (2, 2) scene (Gaussian-spotlight, 1B3H) can be mistaken with the (4, 2) scene (Gaussian-spotlight, 3B1H).

into two groups of 10: G1 (7 male, 3 female, M 22.3, STD 3.0) and G2 (7 male, 3 female, M 23.1, STD 3.1). No participants reported having sensorimotor impairments that could affect experimental results. Each participant was paid 5000 KRW ($\simeq$ 4.5 USD).

5.1.3 Procedure

We used a Senseg Feelscreen as the electrostatic tactile display. An Android application (Fig. 13) was developed using Unity (version 5.32)[30] for both visual and haptic rendering with an update rate of 60 Hz. The sampling rate for tactile signal reconstruction was much higher and determined internally by the Feelscreen library.

Each participant completed two sessions of trials. In the session for the *Visual* task (V), participants were asked to only look at the objects and provide answers as to whether they were bumps or holes. No tactile feedback was provided. In the session for the *Visual + Haptic* task ($\mathsf{V}+H$), participants were told to also touch the objects and then provide their answers. Tactile feedback was presented using our generalized lateral force rendering algorithm.

In the beginning of each session, participants were given enough time to become familiar with the application. For group G1, a session for $\mathsf{V}+H$ was conducted first, followed by a session for V. For group G2, the order was reversed for balanced order. In each session, the 20 scenes were presented to participants once, and their order of presentation

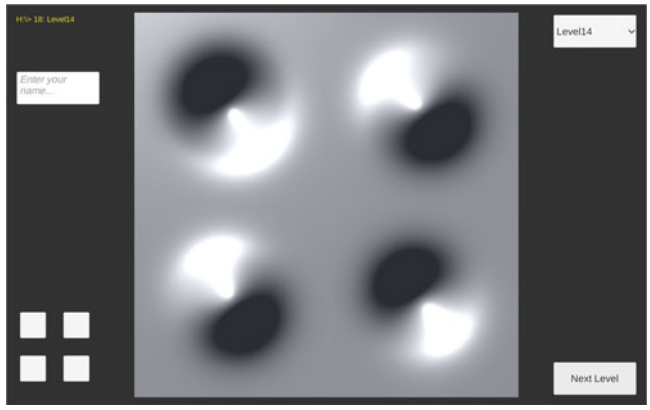

Fig. 13. Snapshot of the GUI program. In the lower right corner, a button was provided to move to the next scene after providing answers using the four toggle buttons in the lower left corner. Participants checked each toggle button for bump and unchecked it for hole, for the corresponding object in the scene.

was randomized for each participant. The experiment took 30 min for each participant.

5.2 Results

We first computed the correct recognition ratios for each participant in each group. A pairwise t-test found no significant difference between the two groups G1 and G2 ($t = 0.14, p = 0.7091$). This suggests that the order of the two sessions did not affect the experimental results. Thus we pooled the data of both groups for further analysis.

The experiment had four independent factors: task (V and $\mathsf{V}+H$), geometry (Gaussian and square frustum), lighting condition (spotlight and directional light), and configuration (0B4H, 1B3H, 2B2H, 3B1H, and 4B0H). For statistical analysis, we applied a four-way within-subject ANOVA, and its results are shown in Table 2.

Task (under different types of sensory feedback), V versus $\mathsf{V}+H$, had a statistically significant effect on the correct recognition ratio with a very small p-value. This can be verified by comparing the mean correct recognition ratios between the two tasks shown in Fig. 14, with 75 versus 95 percent for V and $\mathsf{V}+H$. This result indicates that our shape rendering algorithm using frictional feedback was effective in delivering supplemental shape information when visual rendering alone was not sufficient, improving the correct recognition ratio by 20 percent.

Between the two lighting conditions, spotlight and directional light, a noticeable difference was also reported ($p = 0.0460$). On average, directional light showed higher recognition performance than spotlight with 88 versus 81 percent (Fig. 14 by 7 percent difference. Note, however, the p-value close to the boundary of significance ($\alpha = 0.05$).

Among the many interactions between the main factors, only task $\times$ light was statistically significant ($p = 0.0153$). This means that the two light sources had different effects depending on the task, as shown in Fig. 15. For task V, light was a crucial factor in which directional light achieved higher performance than spotlight with 83 versus 67 percent. However, in task $\mathsf{V}+H$ with the added haptic feedback, light was no longer a main player and both light sources showed very similar performance (96 versus 94 percent). In addition, although the performance was generally improved from task V to $\mathsf{V}+H$, the increase rate was

TABLE 2
Results of Four-Way Within-Subject ANOVA

Factor	F-value	p-value
Task*	$F(1,19) = 27.39$	< 0.0001*
Light*	$F(1,19) = 4.56$	0.0460*
Geometry	$F(1,19) = 0.04$	0.8492
Configuration	$F(4,76) = 1.76$	0.1462
Task × Light*	$F(1,19) = 7.1$	0.0153*
Task × Geometry	$F(1,19) = 0.87$	0.3636
Task × Configuration	$F(4,76) = 0.36$	0.8373
Light × Geometry	$F(1,19) = 1.15$	0.2967
Light × Configuration	$F(4,76) = 0.91$	0.4650
Geometry × Configuration	$F(4,76) = 0.80$	0.5261
Task × Light × Geometry	$F(1,19) = 2.17$	0.1575
Task × Light × Configuration	$F(4,76) = 2.03$	0.0988
Task × Geometry × Configuration	$F(4,76) = 0.68$	0.6084
Light × Geometry × Configuration	$F(4,76) = 1.96$	0.1099
Task × Light × Geometry × Configuration	$F(4,76) = 0.33$	0.8580

approximately 2.5 times larger with spotlight than with directional light. This is another support that the frictional electrovibration feedback was quite effective in rendering 3D shape information.

The other main factors and interaction terms did not have significant effects on the recognition accuracy.

Aside from the main factors, we also investigated how bumps and holes were recognized. The performance difference caused by the two different shapes was negligible (hole 86 versus bump 84 percent). A pairwise t-test did not find a significant effect of bumps and holes on the recognition ratio ($t = 0.91, p = 0.3402$).

5.3 Discussion

Task V + H showed clearly higher performance than task V by the 20 percent improvement of correct recognition with statistical significance. This is due to the additional haptic information provided in task V + H, but not in task V. Therefore, the summative user study provides unequivocal evidence that our generalized lateral force rendering algorithm is effective in rendering 3D shape using electrostatic frictional force.

We could find an interesting observation on the roles of visual and haptic cues. Shading was constant and determined by the position of the objects in the scene with respect to the light source. For example, for bumps, the back faces (from the light source) were always darker than the front faces. This was not the case for haptic feedback since

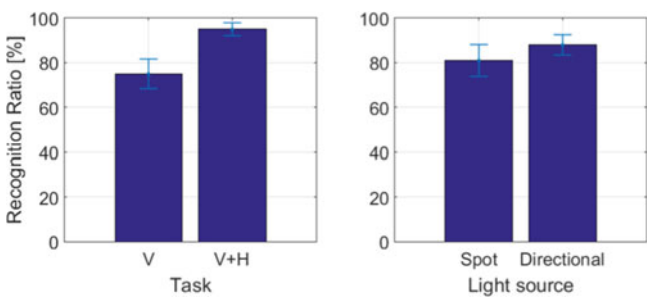

Fig. 14. Correct recognition ratios for task (V 75 percent and V + H 95 percent) and light (spotlight 81 percent and directional 88 percent). Error bars show 95 percent confidence intervals.

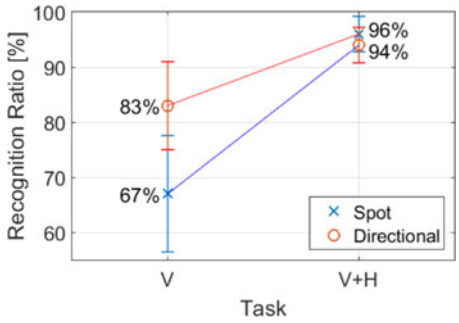

Fig. 15. Interaction effects between task and light. Error bars show 95 percent confidence intervals.

friction changes depended on the scanning direction. In other words, there was no correlation between shade (visual cue) and friction (haptic cue). Depending on the scanning direction, the dark side of a bump could have either large or small friction. This could have created a conflict between the two sensory cues. In spite of this situation, the recognition ratio in task V + H was very high (95 percent). This implies that participants relied more on haptic cues than visual cues to resolve the conflict in sensory information.

We also measured the task completion times for each participant in each trial. They were, on average, 213 s and 427 s for task V and V + H, respectively. This was expected since task V + H required manual scanning on the objects.

6 Conclusion

In this paper, we have presented an effective rendering method for improving the recognition of 3D features rendered on a touchscreen using an electrostatic friction display. First, we carried out a formative user study using a basic gradient-based algorithm adapted from [7] in order to assess users' ability of recognizing primitive 3D shapes based on lateral force feedback provided by an electrostatic tablet and a force-feedback interface. Experimental results demonstrated that users are not able to associate electrovibration patterns with geometric shapes in an absolute manner without contextual information. However, when such guidance was given, participants achieved moderate recognition, and this finding was foundational to our follow-up work. Second, we extended the basic algorithm to support general 3D mesh objects. The generalized algorithm computes the frictional rendering force by estimating the gradient at the touch point and also emphasizes sharp edges on the surface by rendering perceptually salient friction effects. The generalized algorithm is also computationally inexpensive. Lastly, we conducted a summative user study to evaluate the effectiveness of our shape rendering algorithm in reducing the visual uncertainty in 3D shape perception. We found that when frictional feedback was provided, the correct recognition performance was notably increased in comparison to when only visual rendering was presented. To our knowledge, our algorithm is among the first that attempted to improve the perception of 3D shapes modeled using meshes displayed on a touchscreen using electrovibration feedback with acceptable performance.

For future work, we plan to extend this study in two directions: extending the rendering algorithm to support dynamic 3D objects and creating a variable friction display that modulates friction without clear sensations of vibration, which could be more beneficial for our purpose.

ACKNOWLEDGMENTS

This work was supported by a Giga Korea Project (GK15C0100; Development of Interactive and Realistic Massive Giga-Content Technology) of the Ministry of Science, ICT, and Future Planning, Republic of Korea.

REFERENCES

[1] O. Bau, I. Poupyrev, A. Israr, and C. Harrison, "Teslatouch: Electrovibration for touch surfaces," in *Proc. 23nd Annu. ACM Symp. User Interface Softw. Technol.*, 2010, pp. 283–292.
[2] S.-C. Kim, A. Israr, and I. Poupyrev, "Tactile rendering of 3d features on touch surfaces," in *Proc. 26th Annu. ACM Symp. User Interface Softw. Technol.*, 2013, pp. 531–538.
[3] G. Ilkhani, M. Aziziaghdam, and E. Samur, "Data-driven texture rendering with electrostatic attraction," in *Proc. 9th Int. Conf. Human Haptic Sensing Touch Enabled Comput. Appl.*, 2014, pp. 496–504.
[4] Senseg feelscreen development kit. (2015). [Online]. Available: http://www.senseg.com/
[5] Tanvas. (2016). [Online]. Available: http://tanvas.co/
[6] M. Minsky, O.-y. Ming, O. Steele, F. P. Brooks Jr, and M. Behensky, "Feeling and seeing: Issues in force display," *ACM SIGGRAPH Comput. Graph.*, vol. 24, no. 2, 1990, pp. 235–241.
[7] G. Robles-De-La-Torre and V. Hayward, "Force can overcome object geometry in the perception of shape through active touch," *Nature*, vol. 412, no. 6845, pp. 445–448, 2001.
[8] E. Mallinckrodt, A. L. Hughes, and W. Sleator, "Perception by the skin of electrically induced vibrations," *Sci.*, vol. 118, no. 3062, pp. 277–278, 1953.
[9] R. M. Strong and D. E. Troxel, "An electrotactile display," *IEEE Trans. Man-Mach. Syst.*, vol. MMS-11, no. 1, pp. 72–79, Mar. 1970.
[10] D. J. Beebe, C. M. Hymel, K. A. Kaczmarek, and M. E. Tyler, "A polyimide-on-silicon electrostatic fingertip tactile display," in *Proc. IEEE 17th Annu. Conf. Eng. Med. Biol. Soc.*, Sep. 1995, pp. 1545–1546.
[11] 3m microutouch system SCT3250EX (surface capacitive touch technology). (2016). [Online]. Available: http://solutions.3m.com/
[12] D. J. Meyer, M. Peshkin, and J. E. Colgate, "Fingertip friction modulation due to electrostatic attraction," in *Proc. IEEE World Haptics Conf.*, 2013, pp. 43–48.
[13] Y. Zhang and C. Harrison, "Quantifying the targeting performance benefit of electrostatic haptic feedback on touchscreens," in *Proc. Int. Conf. Interactive Tabletops Surfaces*, 2015, pp. 43–46.
[14] H. Kim, J. Kang, K. D. Kim, K. M. Lim, and J. Ryu, "Method for providing electrovibration with uniform intensity," *IEEE Trans. Haptics*, vol. 8, no. 4, pp. 492–496, Oct.-Dec. 2015.
[15] S. Wu, X. Sun, Q. Wang, and J. Chen, "Tactile modeling and rendering image-textures based on electrovibration," *Visual Comput.*, vol. 33, pp. 1–10, 2016.
[16] D. Pyo, S. Ryu, S.-C. Kim, and D.-S. Kwon, "A new surface display for 3D haptic rendering," in *Proc. Int. Conf. Human Haptic Sensing Touch Enabled Comput. Appl.*, 2014, pp. 487–495.
[17] F. Giraud, M. Amberg, and B. Lemaire-Semail, "Merging two tactile stimulation principles: Electrovibration and squeeze film effect," in *Proc. IEEE World Haptics Conf.*, Apr. 2013, pp. 199–203.
[18] E. Vezzoli, M. Amberg, F. Giraud, and B. Lemaire-Semail, "Electrovibration modeling analysis," in *Haptics: Neuroscience, Devices, Modeling, and Applications*. Berlin, Germany: Springer, 2014, pp. 369–376.
[19] H. Haga, K. Yoshinaga, J. Yanase, D. Sugimoto, K. Takatori, and H. Asada, "Electrostatic tactile display using beat phenomenon of voltage waveforms," in *Proc. SID Symp. Digest Technical Papers*, 2014, pp. 623–626.
[20] T. Nakamura and A. Yamamoto, "Multi-finger electrostatic passive haptic feedback on a visual display," in *Proc. IEEE World Haptics Conf.*, 2013, pp. 37–42.
[21] C. D. Shultz, M. A. Peshkin, and J. E. Colgate, "Surface haptics via electroadhesion: Expanding electrovibration with Johnsen and Rahbek," in *Proc. IEEE World Haptics Conf.*, 2015, pp. 57–62.
[22] D. Wijekoon, M. E. Cecchinato, E. Hoggan, and J. Linjama, "Electrostatic modulated friction as tactile feedback: Intensity perception," in *Haptics: Perception, Devices, Mobility, and Communication*. Berlin, Germany: Springer, 2012, pp. 613–624.
[23] J. Kang, H. Kim, S. Choi, K. D. Kim, and J. Ryu, "Investigation on low voltage operation of electrovibration display," *IEEE Trans. Haptics*, vol. PP, no. 99, 2017.
[24] Y. Vardar, B. Güçlü, and C. Basdogan, "Effect of waveform in haptic perception of electrovibration on touchscreens," in *Proc. Int. Conf. EUROHAPTICS*, 2016, pp. 190–203.
[25] R. H. Osgouei, J. R. Kim, and S. Choi, "Identification of primitive geometrical shapes rendered using electrostatic friction display," in *Proc. IEEE Haptics Symp.*, 2016, pp. 198–204.
[26] D. A. Forsyth and J. Ponce, Computer vision: A modern approach. Prentice Hall Professional Technical Reference, 2002.
[27] R. Maini and H. Aggarwal, "Study and comparison of various image edge detection techniques," *Int. J. Image Process.*, vol. 3, no. 1, pp. 1–11, 2009.
[28] X. Yang, J. Zheng, and D. Wang, "A computational approach to joint line detection on triangular meshes," *Eng. Comput.*, vol. 30, no. 4, pp. 583–597, 2014.
[29] A. Hubeli, K. Meyer, M. H. Gross, M. H. Gross, and M. H. Gross, *Mesh Edge Detection.* Swiss Federal Institute of Technology, Department of Computer Science, Institute of Scientific Computing, Computer Graphics Group, Zürich, Switzerland, 2000.
[30] Unity - game engine. (2016). [Online]. Available: http://www.unity3d.com

Reza Haghighi Osgouei received the BSc and MSc degrees in electrical engineering: control systems from the Sahand University of Technology, Tabriz, Iran, and the Amirkabir University of Technology, Tehran, Iran, in 1999 and 2003, respectively. He received the second MSc degree in computer science and engineering from POSTECH, Pohang, Rep. of Korea, in 2012. Since 2013, he has been working toward the PhD degree in the Department of Computer Science and Engineering at POSTECH. He has been working on surface haptics, more focused on rendering surface 3D curvature and texture on electrovibration display. He is a student member of the IEEE.

Jin Ryong Kim received the BS and MS degrees in electrical and computer engineering from Hanyang University, Seoul, Korea, in 2001 and 2004, respectively, and the MS degree in computer science from Purdue University, West Lafayette, IN, in 2010. He received the PhD degree in electrical and computer engineering from Purdue University, in 2014. He is currently a senior researcher at the Electronics and Telecommunications Research Institute (ETRI) in Korea. His current research interests include haptics, HCI, and UI/UX, but more focused on creating novel interaction through haptic technology. He is a member of IEEE.

Seungmoon Choi received the BS and MS degrees in control and instrumentation engineering from Seoul National University, in 1995 and 1997, respectively, and the PhD degree in electrical and computer engineering from Purdue University in 2003. He is a professor of computer science and engineering with the Pohang University of Science and Technology (POSTECH). He received a 2011 Early Career Award from the IEEE Technical Committee on Haptics and several best paper awards from major international conferences. He was a co-chair of the IEEE Technical Committee on Haptics in 2009-2010. He serves/served on the editorial board of the *IEEE Transactions on Haptics*, *Presence*, *Virtual Reality*, and the *IEEE Robotics and Automation Letters*. He was the general co-chair of IEEE Haptics Symposium in 2014 and 2016 and the program chair of IEEE World Haptics 2015. His research interests lie on haptic rendering and perception, both in kinesthetic and tactile aspects. His basic research has been applied to mobile devices, automobiles, virtual prototyping, and motion-based remote controllers. He is a senior member of the IEEE.